



Article

Sustainable Manufacture of Natural Fibre Reinforced Epoxy Resin Composites with Coupling Agent in the Hardener

Aitor Hernandez Michelena^{1,2}, John Summerscales^{3,*} , Jasper Graham-Jones³ and Wayne Hall⁴

¹ 5'TX", Arotz Kalea 15, 20800 Zarautz, Spain; 5txsurfs@gmail.com

² Siemens Gamesa Renewable Energy, C. Soto Aizoain, 2-168, 56, 31013 Pamplona, Spain

³ MAterials and STructures (MAST) Research Group/Composites Engineering, School of Engineering, Computing and Mathematics (SECaM), Reynolds Building, University of Plymouth, Plymouth PL4 8AA, UK; jasper.graham-jones@plymouth.ac.uk

⁴ Griffith School of Engineering and Built Environment, Griffith University, Southport, QLD 4222, Australia; w.hall@griffith.edu.au

* Correspondence: j.Summerscales@plymouth.ac.uk; Tel.: +44-1752-5-86150

Abstract: Lignocellulosic natural fibres are hydrophilic, while many matrix systems for composites are hydrophobic. The achievement of good mechanical properties for natural fibre-reinforced polymer (NFRP) matrix composites relies on good fibre-to-matrix bonding at the interface. The reinforcement is normally coated with an amphiphilic coupling agent to promote a strong interface. A novel alternative approach is to dissolve the coupling agent in the hardener for the resin before creating the stoichiometric mix with the base epoxy resin. During composite manufacture, the hydrophilic (polar) end of the coupling agent migrates to surfaces (internal interfaces) and bonds to the fibres. The hydrophobic (non-polar) end of the coupling agent remains embedded in the mixed resin. Mechanical testing of composite samples showed that silane added directly to the matrix produced a NFRP composite with enhanced longitudinal properties. As pre-process fibre coating is no longer required, there are economic (shorter process times), environmental (elimination of contaminated solvents) and social (reduced worker exposure to chemical vapours) benefits arising from the new technique.

Keywords: coupling agent; epoxy resin; hardener; interface; natural fibre



Citation: Hernandez Michelena, A.; Summerscales, J.; Graham-Jones, J.; Hall, W. Sustainable Manufacture of Natural Fibre Reinforced Epoxy Resin Composites with Coupling Agent in the Hardener. *J. Compos. Sci.* **2022**, *6*, 97. <https://doi.org/10.3390/jcs6030097>

Academic Editors:
Mohamed Ragoubi,
Frédéric Becquart and
Ahmed Koubaa

Received: 26 February 2022

Accepted: 13 March 2022

Published: 18 March 2022

Publisher's Note: MDPI stays neutral with regard to jurisdictional claims in published maps and institutional affiliations.



Copyright: © 2022 by the authors. Licensee MDPI, Basel, Switzerland. This article is an open access article distributed under the terms and conditions of the Creative Commons Attribution (CC BY) license (<https://creativecommons.org/licenses/by/4.0/>).

1. Introduction

Natural fibre-reinforced polymer (NFRP) matrix composites can potentially contribute to the Sustainable Development Goals: 8 Decent Work and Economic Growth, 9 Industry, Innovation and Infrastructure and 12 Responsible Consumption and Production. All claims to sustainability should be validated by a quantitative Life Cycle Assessment (QLCA). There are many reviews dedicated to NFRP, e.g., [1–10], and the Virtual Book on Bast Fibres and Their Composites is a bibliography listing over 300 books, chapters, and review papers on NFRP [11].

The achievement of good mechanical properties requires effective load transfer between the matrix and the composite. The Cox shear-lag model [12,13] is a representation of the transfer of load between the matrix and the reinforcement fibres by interfacial shear stresses. The model uses a fibre length distribution factor (FLDF) to indicate the efficiency of load transfer. FLDF (η_l) assumes that (i) the matrix and fibre remain elastic, and the interface bond is perfect, (ii) the shear stress at the fibre ends is maximum and falls to zero after half the “critical length”, and (iii) the tensile stress at the fibre ends is zero and rises to a maximum after half the “critical length”. FLDF for circular cross-section fibres is calculated using Equation (1), where Equation (2) expands the β term:

$$\eta_l = 1 - \frac{\tanh(\beta L/2)}{\beta L/2} \quad (1)$$

$$\beta = \frac{2 \pi G_m}{E A \ln (R/R_f)} \quad (2)$$

where A_f is the cross-sectional area of the fibre, G_m is the shear modulus of the matrix, L is the fibre length, R_f is the radius of the fibre and R is the mean separation of the fibres. For natural fibres, the cross-sectional area is normally calculated from a transverse measurement of apparent diameter and an incorrect assumption of circular cross-section. Virk et al. [14] have proposed a Fibre Area Correction Factor, FACF (κ), for natural fibres. Determination of the “the mean separation of the fibres” is a non-trivial task for real materials.

If the fibre is shorter than the critical length (l_c), it will never carry a load high enough to cause fibre fracture. The composite will instead fail in shear, either at the fibre/matrix interface or in the matrix itself. Nayfeh [15] and McCartney [16] have proposed alternative equations for the prediction of β . Nairn [17,18] generalised the shear lag analysis to permit modelling of imperfect interfaces between concentric cylinders and, with Mendels [19], within multilayered structures.

Given that the shear lag analysis requires that the interface bond is perfect, it is normal to enhance the fibre-to-matrix bond. Various pretreatments for natural fibre reinforcements have been considered for their potential to enhance the interfacial bond and hence the properties of the composites. The processes are summarised in Table 1 and may be used individually or in combination.

Table 1. Pretreatment process to enhance interfacial adhesion between the reinforcement fibre and the matrix [20–27].

Process	Characteristics	Reference
Nanocellulose	deposition of bacterial products	[28,29]
Enzymes	natural chemicals that catalyse reactions	[30–33]
Coupling agents	chemicals with differing functionality at each end	[20–23]
Esterification	reaction with organic acids or anhydrides (e.g., acetylation with acetic acid)	
Grafting	generation of side chains, e.g., maleation with maleic anhydride, or cyanoethylation with acrylonitrile	
Mercerisation	treatment with a concentrated solution of caustic alkali	
Surface oxidation	treatment with, e.g., potassium permanganate	
Plasma treatment	treatment with ionised gas	[34]
Ultraviolet	for example, 2 kW UV (133–254 nm wavelength) radiation	[35]
Ionic liquids	combinations of organic cations and inorganic or organic anions, which are molten salts below 100 °C.	[36]

Mercerisation [37] is defined as the “treatment of cellulosic textiles in yarn or fabric form with a concentrated solution of caustic alkali [soda], whereby the fibres are swollen, the strength and dye affinity of the materials are increased, and their handle is modified. The process takes its name from its discoverer, John Mercer (1844)”. The treatment removes practically all non-cellulose components except waxes and changes the crystal structure of the cellulose. Mercerisation results in “hydrated cellulose”, which is chemically identical to the precursor material but has different physical properties [38]. Mercerisation converts cellulose I to $50 \pm 15\%$ cellulose II with a consequent expansion of the crystal lattice [39] as adjacent chains move further apart. This change explains the greater chemical reactivity and increased water absorption of mercerised cellulose [1]. For rapeseed straw, Paukszta [40] has shown optimal conditions for the process to be solution concentrations in the range 12.5–20% for >5 min.

The most common form of coupling agent (CA) is a “silane” (the simplest silane is silicon tetrahydride, SiH_4). For composite interfaces, the CA is normally an amphiphilic molecule with a non-polar chain with one end having a reactive moiety to link to the resin (e.g., vinyl silane for unsaturated polyester or vinyl ester resins, or epoxy silane for epoxy resins) and the silane moiety at the other end attaches to the fibre. There are

reviews of coupling agents used for polymer matrix composites [20], and for the specific case of natural fibre reinforcements [21–23]. Typical silane coupling agents include APS (3-aminopropyltrimethoxysilane), MPS (γ -methacryloxypropyltrimethoxy silane), and VTMO (vinyltrimethoxysilane).

Hand et al. [41] reported the use of a resin formulation with γ -glycidoxypropyltrimethoxy silane mixed into a bisphenol A/F blend with polyamidoamine hardener to strengthen glass microscope slides. The authors of this paper have not identified research where coupling agents for composites have been added to the resin system rather than used to treat the fibres. The approach adopted for the study reported in this paper is to dissolve the coupling agent in the hardener for the resin system. This process change should lead to the elimination of the separate solution treatment of the fibres, and in turn, to reduce the costs, the worker exposure to chemicals, and the environmental burdens of the fibre processing, leading to more sustainable manufacture of the composites.

2. Materials and Methods

Preliminary experiments to establish optimum working conditions are reported in Hernandez Michelena [42].

The fibre reinforcement used in this study was Composites Evolution (Chesterfield, England) Biotex Flax 275 gsm unidirectional twistless fabric and was assumed to have no surface treatment [43]. The flax fibre properties (from the supplier datasheet with no statistical information) were average flax fibre apparent diameter (measured under an optical microscope and assuming circular cross-section) 20 μm , fibre density 1500 kg/m^3 . The resin system was Huntsman LLC (The Woodlands, TX, USA) Araldite LY 1568 CH/Aradur 3489 CH petrochemical-based epoxy [44]. The base resin was bisphenol A epoxy resin (CAS # 25068-38-6) with ~10% dodecyl and tetradecyl glycidyl ethers (CAS # 68609-97-2). Aradur 3489 is a polyamine hardener with “a very long open time at room temperature” (gel time~900 min) [45]. A 100:28 mixture of the resin and hardener by weight has an initial viscosity of 200–300 mPa s at 25 $^\circ\text{C}$ (supplier data using ISO12058). The mechanical properties of the fibres and resin are given in Table 2. The coupling agent was 3-aminopropyltrimethoxysilane, $(\text{CH}_3\text{O})_3\text{Si}(\text{CH}_2)_3\text{NH}_2$, (APS from BYK-Chemie GmbH BYK-C 8001, Wesel, Germany; CAS #13822-56-5; molecular weight 179.29) as a viscous liquid, specifically developed for glass fibre-reinforced epoxy resin composites (Figure 1). Sodium hydroxide (NaOH; CAS #1310-73-2; molecular weight 40; granules) and ethanol ($\text{C}_2\text{H}_5\text{OH}$; CAS #64-17-5; molecular weight 46.07; thin clear liquid) were from Sigma-Aldrich (St. Louis, MO, USA).

Table 2. Modulus, strength and strain to failure of the reinforcement and matrix [43,44].

Materials	Tensile Modulus (GPa)	Tensile Strength (MPa)	Strain at Failure (%)
Biotex Flax 275 gsm UD Twistless Technology fabric	50	500	2.0
Araldite LY1568 CH/Aradur 3489 CH epoxy	2.92	69	10.75

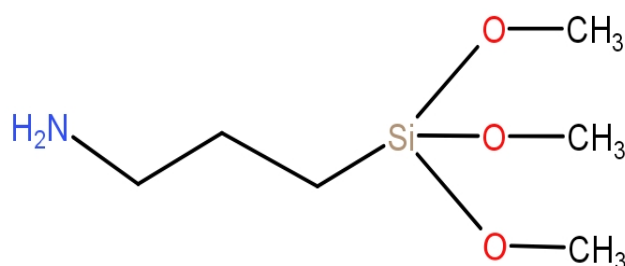


Figure 1. 3-aminopropyltrimethoxysilane coupling agent.

Each batch of fibres was subjected to one of four treatments (Table 3) before composites manufacture, where the codes are M mercerised fibre, S silane in hardener, U untreated fibre, Z exposed to silane solution but Zero silane in hardener.

Table 3. Fibre treatment processes applied before composite manufacture.

Code	Materials	Silane in Hardener
US	untreated fibre	1.5%
MS	mercerised fibre (3 h at 1 M NaOH).	1.5%
UZ	untreated fibre exposed to 1% silane solution (equal parts water and ethanol) for 1 h at ambient temperature, then dried at ambient temperature for 48 h.	×
MZ	mercerised fibre (3 h at 1 M NaOH) exposed to 1% silane solution (equal parts water and ethanol) for 1 h at ambient temperature, then dried at ambient temperature for 48 h.	×

Composites plates of 330 mm (transverse to flow) by 600 mm long were produced using four (4) layers of reinforcement on an AMOND lamination table by resin infusion under flexible tooling with a flow medium (RIFT II) [46,47]. The process consumables were AeroFilm® VB160 vacuum bag, AeroFilm® PP230 peel ply, AeroFilm® FM105 flow mesh, Resin infusion spiral medium flow coil, 12.7 mm internal diameter wire reinforced vacuum hose, and vacuum bagging gum sealant tacky tape. A porous membrane appropriate to the Airbus Defence and Space GmbH (formerly EADS) patented Vacuum Assisted Process (VAP®) was used (description commercially sensitive) [48]. The resin was preheated for 30 min at 40 °C before infusion. The composites were cured in an electrically heated mould tool for 2 h at 65 °C, 1 h at 80 °C and 1 h at 100 °C.

Tensile tests were conducted in accordance with ISO527-4/-5 standards with 10 samples for each condition and thickness between 2 and 10 mm. Samples were 250 mm long with a 150 mm free length between the tabs and 15 mm (longitudinal) or 25 mm (transverse) wide. The tabs were ±45° glass fibre epoxy (two layers of 1200 gsm biaxial fabric) adhered with Araldite 2015 bi-component epoxy adhesive and cured for 1 h at ambient temperature then post-cured for 1 h at 60 °C. Samples were cut using a Mutronic DIADISC 5200R cutting machine with a hard steel saw blade (high thermal conductivity to avoid burning the samples). Mechanical testing was performed on a Shimadzu AG-X PLUS 250KN universal testing machine with a 100 kN load cell (using Trapezium X software and accuracy class 0.5 according to UNE-EN-ISO-7500-1:2006) at a crosshead speed of 2 mm/min. Strains were measured by video extensometers. The test climate was in compliance with ISO291 class 2.

3. Results

The CRAG test 1000 [49] for the assessment of fibre volume fraction (FVF) by the thickness measurement method uses Equation (3):

$$V_f = n A_F / \rho_f t \tag{3}$$

where V_f is the volume fraction of fibres, n is the number of layers, A_F is the areal weight of the fabric, ρ_f is the density of the fibre, and t is the thickness of the plate. For the determination of V_f , the mean value for either longitudinal (14 samples) or transverse (9 samples) thickness is calculated, then an average of the two values is used. The transverse thickness is marginally higher than the longitudinal value due to the sampling position relative to the flow direction.

Virk et al. [14] presented extended rules-of-mixture for the estimation of the tensile modulus (Equation (4)) and for the axial tensile strength of unidirectional natural fibre reinforced composites (Equation (5)):

$$E_c = \kappa \eta_d \eta_l \eta_o V_f E_f + V_m E_m \tag{4}$$

$$\sigma_c' = \kappa V_f \sigma_f' + V_m \sigma_{m*} \tag{5}$$

where subscript x is c , f , m or v for composite, fibre, matrix or voids, respectively. E_x = Young's modulus of the material indicated by the subscript. V_x = volume fraction ($V_f + V_m + V_v = 1$). κ = fibre area correction factor (FACF). η_d = fibre diameter distribution factor, η_l = fibre length distribution factor, and η_o = fibre orientation distribution factor. σ_x' is a material strength, and σ_{m*} is the stress in the matrix at the failure strain of the fibre (calculated as 12.84 MPa).

Table 4 presents the experimental longitudinal and transverse tensile properties for the four batches of samples. The fibre volume fractions for the solution processed (MS, UZ, MZ) plates are derived using Equation (3) with the unswollen fibre density. The final four rows show the estimated values (i.e., normalised for FVF) for the axial moduli and strengths using material properties from Table 2 and Equation (4) or Equation (5), respectively. The values for κ , η_d , η_l and η_o were all set at unity (1) given no agreement on FACF values for flax [50], fibres characterised at the diameter used, the long flax fibres are above the critical length, and all fibres are assumed to be globally oriented along the test axis with no local waviness, respectively.

Table 4. Longitudinal and transverse tensile properties for flax fibre composites with different fibre treatments and the addition (or not) of silane in the hardener.

Property (Plate Number)	US (25)	MS (26)	UZ (27)	MZ (28)
Mercerised	✗	✓	✗	✓
Silane solution	✗	✗	✓	✓
Silane in hardener	✓	✓	✓	✗
Mean thickness (mm) 0°/90°	2.26/2.32	3.14/3.31	2.66/2.73	2.93/3.19
Fibre volume fraction (%)	32.0	22.7	27.2	24.0
Axial modulus (GPa)	14.18 ± 2.04	7.85 ± 1.19	9.24 ± 0.68	9.06 ± 0.82
Transverse modulus (GPa)	3.66 ± 0.51	4.08 ± 0.45	3.72 ± 0.54	3.87 ± 0.30
Axial strength (MPa)	157.6 ± 4.7	85.9 ± 1.9	116.6 ± 2.7	91.5 ± 5.5
Transverse strength (MPa)	18.27 ± 0.74	16.48 ± 1.08	20.99 ± 1.58	22.24 ± 1.35
Axial strain at failure (%)	1.54 ± 0.07	1.75 ± 0.12	1.61 ± 0.08	1.55 ± 0.17
Transverse strain at failure (%)	0.55 ± 0.09	0.44 ± 0.05	0.59 ± 0.07	0.65 ± 0.07
Predicted elastic modulus (GPa)	17.97	13.61	15.76	14.22
Modulus (experimental/predicted)	79%	58%	59%	64%
Predicted strength (MPa)	169	129	145	130
Strength (experimental/prediction)	93%	67%	80%	71%

All experimental properties are lower than the respective predictions as expected for imperfect materials. The material properties from supplier data sheets may be optimistic and not recognise deterioration due to packing, transport, storage and handling. The fibres exceed the critical length but are not continuous. The fibre orientation is likely to be off-axis globally and with local waviness. Further, resin-rich volumes (RRV), which inevitably increase with increasing matrix volume fraction, lead to a disproportionate decrease in composite strength [51].

4. Discussion

The composites processed with silane-in-hardener are significantly thinner than the other three laminates and hence have higher fibre volume fraction. The expansion of the crystal lattice [39] during mercerisation will increase the volume of the fibre. Residual swelling in the solution treated fibres leads to them occupying a greater volume. Lu et al. [52] have reported that flax technical fibres exhibit a higher degree of swelling in moist environments than the elementary fibres in the 5–90% relative humidity range. Further, the surface friction may be changed so that fabric compressibility characteristics are different.

The amine group in the coupling agent is likely to act as a curing agent for the epoxy resin and to dissolve into the bulk resin. The methoxy group (CH_3O^-) is unlikely to react with the epoxy and is likely to migrate to surfaces. The fibre-matrix interface in a high fibre volume fraction composite will be distributed through the material, so migration distances to a fibre surface will be short.

Khanjanzadek et al. [53] and Kono et al. [54] have inferred that the APS coupling agent reacts with an alcohol group on the surface of cellulose to form an ether linkage to the substrate and release methanol (CH_3OH). Each coupling agent molecule has triple methoxy groups, so the linkage can form at three sites. The strong coupling between the fibre reinforcement and the resin matrix should result in good axial and transverse properties.

The axial tensile modulus and strength obtained for samples manufactured with untreated fibres with the silane coupling agent mixed into the hardener were statistically well above those obtained for the other treatments (Figures 2 and 3). The effective transfer of axial load between the matrix and the fibres is accompanied by low transverse properties.

However, the properties achieved will be a function of fibre volume fraction. To confirm the benefits of the coupling agent into the hardener process, the experimental data were referenced to the Virk predictions. The new coupling agent in hardener (CAH) technique is confirmed as giving the highest mechanical properties pro rata to fibre volume fraction.

Future work might consider the modification of Equations (1) and (2) for the shear lag load transfer. However, two parameters are problematic. R_f , the radius of the fibre needs to account for the non-circular cross-section of natural fibres, probably by use of an apparent diameter and/or a fibre area correction factor [14]. R , the mean separation of the fibres, is even less tractable. If the fibres are assumed to be perfectly parallel, and of constant cross-section, then optical micrographs reflecting the morphology of the composites could provide data on the centroids for each individual fibre. Point processes (e.g., nearest neighbour indices or chi-squared indices) might then permit definition of the mean separation [55]. Alternative procedures for the characterisation of spatial distributions include tessellation and fractal dimension [56]. However, both the resin and the fibres are translucent, so it is difficult to obtain good contrast in optical microscopy, especially over an area adequate for good statistical data. Dyed fibres (but beware changes to fibre structure in aqueous solution) and/or pigmented resin could enhance contrast.

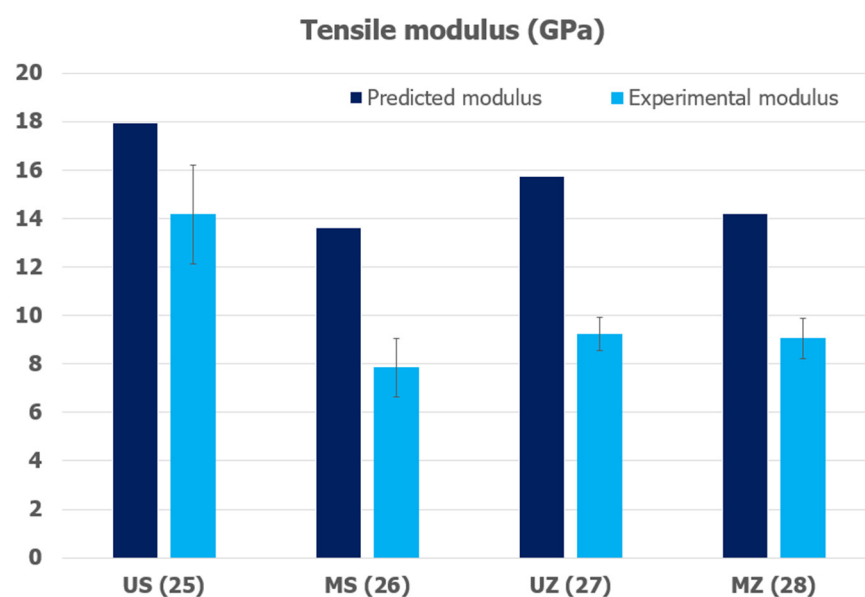


Figure 2. Predicted and experimental axial moduli for the four conditions. M = mercerised, S = silane in hardener, U = not mercerised, Z = no silane in hardener.

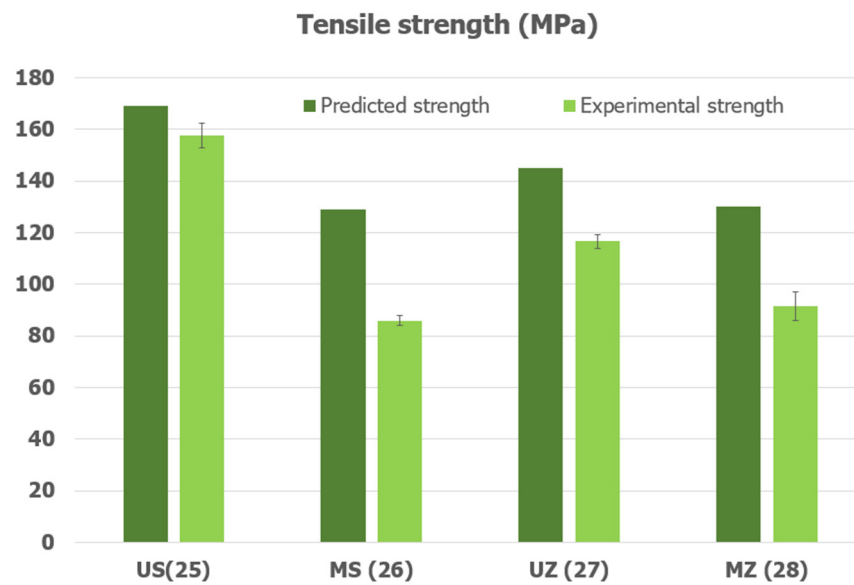


Figure 3. Predicted and experimental axial strengths for the four conditions M = mercerised, S = silane in hardener, U = not mercerised, Z = no silane in hardener.

X-ray computed tomography may provide an alternative route to the data, but most current systems have voxel resolution of a similar magnitude to the radius of the fibre. Further, the density of the resin ($\sim 1200 \text{ kg m}^{-3}$) and fibre ($\sim 1500 \text{ kg m}^{-3}$) is too close for good x-ray contrast. Depriester et al. [57] have recently presented an algorithm for individual fibre separation in 3D fibrous materials imaged by X-ray tomography.

Future work should also consider validating the idea with Life Cycle Assessment to quantify the environmental burdens and the benefits of the process.

The incorporation of the coupling agent into the hardener will potentially improve the sustainability of the system through elimination of the two-step treatment of the fibre by mercerisation then immersion in silane solution. The chemicals involved in fibre treatment inevitably incur a waste stream which could lead to potential pollution of ecosystems. Further process times are reduced, and worker safety is enhanced, by elimination of the treatment processes.

Adoption of silane-in-hardener for the manufacture of natural fibre reinforced epoxy matrix composites could potentially contribute to the United Nations Sustainable Development Goals (SDG):

8: Decent work and economic growth (reduced exposure to chemicals and lower process costs),

9: Industry, innovation and infrastructure (improved component performance), and

12: Responsible consumption and production (reduced chemical pollution).

5. Conclusions

Incorporation of coupling agent in hardener (CAH), rather than prior treatment of the reinforcement, potentially improves the sustainability of the manufacturing process. The specific benefits are reduced worker exposure to aggressive chemicals, fewer process steps leading to reduced costs, and elimination of pollution by waste chemicals.

The longitudinal tensile modulus and strength of the composite are improved by the CAH procedure. The transverse properties retain comparable values to those for composites manufactured by alternative techniques.

Author Contributions: Conceptualization, A.H.M.; methodology, A.H.M.; formal analysis, A.H.M.; investigation, A.H.M.; resources, A.H.M. and J.S.; writing—original draft preparation, A.H.M. and J.S.; writing—review and editing, A.H.M., J.S., J.G.-J. and W.H.; supervision, J.S., J.G.-J. and W.H.;

project administration, J.S.; funding acquisition, A.H.M. All authors have read and agreed to the published version of the manuscript.

Funding: This research was partially funded by a Santander Postgraduate Internationalisation Scholarship.

Data Availability Statement: The data presented in this study are openly available in the Plymouth Electronic Archive and Research Library (PEARL), Available online: <https://hdl.handle.net/10026.1/14297>, accessed on 12 March 2022.

Acknowledgments: The work was mainly conducted in the Basque Country (Euskadi) in northern Spain using facilities in the University of the Basque Country (UPV/EHU), University of Zaragoza and Acciona (latterly Nordex) Windpower in Sariguren. The authors would especially like to thank Brendon Weager at Composites Evolution for reinforcement fabrics and Jaime Ferrer-Dalmau at Entropy Resins for the bio-epoxy. Preliminary results from this study were presented as paper 275 at the 3rd International Conference on Natural Fibers, Braga, Portugal, 21–23 June 2017 and an extended abstract in Procedia Engineering.

Conflicts of Interest: The authors declare no conflict of interest. The funders had no role in the design of the study; in the collection, analyses, or interpretation of data; in the writing of the manuscript, or in the decision to publish the results.

References

1. Dąbrowska, A. Plant-Oil-Based Fibre Composites for Boat Hulls. *Material* **2022**, *15*, 1699. [CrossRef]
2. Fitzgerald, A.; Proud, W.; Kandemir, A.; Murphy, R.J.; Jesson, D.A.; Trask, R.S.; Hamerton, I.; Longana, M.L. A Life Cycle Engineering Perspective on Biocomposites as a Solution for a Sustainable Recovery. *Sustainability* **2021**, *13*, 1160. [CrossRef]
3. Gholampour, A.; Ozbakkaloglu, T. A review of natural fiber composites: Properties, modification and processing techniques, characterization, applications. *J. Mater. Sci.* **2020**, *55*, 829–892. [CrossRef]
4. Hill, C.; Hughes, M. Natural Fibre Reinforced Composites Opportunities and Challenges. *J. Biobased Mater. Bioenergy* **2010**, *4*, 148–158. [CrossRef]
5. Pickering, K.L.; Efendy, M.G.A.; Le, T.M. A review of recent developments in natural fibre composites and their mechanical performance. *Compos. Part A Appl. Sci. Manuf.* **2016**, *83*, 98–112. [CrossRef]
6. Sadrmanesh, V.; Chen, Y. Bast fibres: Structure, processing, properties, and applications. *Int. Mater. Rev.* **2019**, *64*, 381–406. [CrossRef]
7. Sanivada, U.K.; Mármol, G.; Brito, F.P.; Fangueiro, R. PLA Composites Reinforced with Flax and Jute Fibers—A Review of Recent Trends, Processing Parameters and Mechanical Properties. *Polymers* **2020**, *12*, 2373. [CrossRef]
8. Shah, D.U. Developing plant fibre composites for structural applications by optimising composite parameters: A critical review. *J. Mater. Sci.* **2013**, *48*, 6083–6107. [CrossRef]
9. Syduzzaman, M.; Al Faruque, A.; Bilisik, K.; Naebe, M. Plant-Based Natural Fibre Reinforced Composites: A Review on Fabrication, Properties and Applications. *Coatings* **2020**, *10*, 973. [CrossRef]
10. Zwawi, M. A Review on Natural Fiber Bio-Composites; Surface Modifications and Applications. *Molecules* **2021**, *26*, 404. [CrossRef]
11. Summerscales, J. Virtual Book on Bast Fibres and Their Composites. Available online: https://ecm-academics.plymouth.ac.uk/jsummerscales/mats347/bast_book.htm (accessed on 11 March 2022).
12. Cox, H.L. The elasticity and strength of paper and other fibrous materials. *Br. J. Appl. Phys.* **1952**, *3*, 72–79. [CrossRef]
13. Folkes, M.J. *Short Fibre Reinforced Thermoplastics*; Research Studies Press: Letchworth, UK, 1982; ISBN 0-471-10209-1.
14. Virk, A.S.; Hall, W.; Summerscales, J. Modulus and strength prediction for natural fibre composites. *Mater. Sci. Technol.* **2012**, *28*, 864–871. [CrossRef]
15. Nayfeh, A.H. Thermomechanically induced interfacial stresses in fibrous composites. *Fibre Sci. Technol.* **1977**, *10*, 195–209. [CrossRef]
16. McCartney, L.N. Analytical models of stress transfer in unidirectional composites and cross-ply laminates, and their application to the prediction of matrix/transverse cracking. In Proceedings of the IUTAM Symposium on Local Mechanics Concepts for Composite Material Systems, Blacksburg, VA, USA, 27–31 October 1992; Reddy, J.N., Reifsnider, K.L., Eds.; Springer: Berlin, Germany, 1992; pp. 251–282, ISBN 3-540-55547-1.
17. Nairn, J.A. Generalized Shear-Lag Analysis Including Imperfect Interfaces. *Adv. Compos. Lett.* **2004**, *13*, 263–274. [CrossRef]
18. Nairn, J.A. On the use of shear-lag methods for analysis of stress transfer in unidirectional composites. *Mech. Mater.* **1997**, *26*, 63–80. [CrossRef]
19. Nairn, J.; Mendels, D. On the use of planar shear-lag methods for stress-transfer analysis of multilayered composites. *Mech. Mater.* **2001**, *33*, 335–362. [CrossRef]
20. Shokoohi, S.; Arefazar, A.; Khosrokhavar, R. Silane Coupling Agents in Polymer-based Reinforced Composites: A Review. *J. Reinf. Plast. Compos.* **2008**, *27*, 473–485. [CrossRef]

21. Lu, J.Z.; Wu, Q.; McNabb, H.S. Chemical coupling in wood fibre and polymer composites: A review of coupling agents and treatments. *Wood Fiber Sci.* **2000**, *32*, 88–104. Available online: <https://www.researchgate.net/publication/280136866> (accessed on 11 March 2022).
22. Xie, Y.; Hill, C.A.S.; Xiao, Z.; Militz, H.; Mai, C. Silane coupling agents used for natural fiber/polymer composites: A review. *Compos. Part A Appl. Sci. Manuf.* **2010**, *41*, 806–819. [[CrossRef](#)]
23. Anbupalani, M.S.; Venkatachalam, C.D.; Rathanasamy, R. Influence of coupling agent on altering the reinforcing efficiency of natural fibre-incorporated polymers—A review. *J. Reinf. Plast. Compos.* **2020**, *39*, 520–544. [[CrossRef](#)]
24. Liu, M.; Thygesen, A.; Summerscales, J.; Meyer, A.S. Targeted pre-treatment of hemp bast fibres for optimal performance in biocomposite materials: A review. *Ind. Crop. Prod.* **2017**, *108*, 660–683. [[CrossRef](#)]
25. Burrola-Núñez, H.; Herrera-Franco, P.J.; E Rodríguez-Félix, D.; Soto-Valdez, H.; Madera-Santana, T.J. Surface modification and performance of jute fibers as reinforcement on polymer matrix: An overview. *J. Nat. Fibers* **2019**, *16*, 944–960. [[CrossRef](#)]
26. Koohestani, B.; Darban, A.K.; Mokhtari, P.; Yilmaz, E.; Darezereshki, E. Comparison of different natural fiber treatments: A literature review. *Int. J. Environ. Sci. Technol.* **2019**, *16*, 629–642. [[CrossRef](#)]
27. Latif, R.; Wakeel, S.; Khan, N.Z.; Siddiquee, A.N.; Verma, S.L.; Khan, Z.A. Surface treatments of plant fibers and their effects on mechanical properties of fiber-reinforced composites: A review. *J. Reinf. Plast. Compos.* **2018**, *38*, 15–30. [[CrossRef](#)]
28. Kalia, S.; Thakur, K.; Celli, A.; Kiechel, M.A.; Schauer, C.L. Surface modification of plant fibers using environment friendly methods for their application in polymer composites, textile industry and antimicrobial activities: A review. *J. Environ. Chem. Eng.* **2013**, *1*, 97–112. [[CrossRef](#)]
29. Lee, K.-Y.; Delille, A.; Bismarck, A. Greener surface treatments of natural fibres for the production of renewable composite materials. In *Cellulose Fibers: Bio- and Nano-Polymer Composites—Green Chemistry and Technology*; Kalia, S., Kaith, B.S., Kaur, I., Eds.; Springer: Heidelberg, Germany, 2011; ISBN 978-3-642-17369-1. [[CrossRef](#)]
30. Madhu, A.; Chakraborty, J. Developments in application of enzymes for textile processing. *J. Clean. Prod.* **2017**, *145*, 114–133. [[CrossRef](#)]
31. Sisti, L.; Totaro, G.; Vannini, M.; Celli, A. Retting process as a pretreatment of natural fibers for the development of polymer composites. In *Lignocellulosic Composite Materials*; Kalia, S., Ed.; Springer: Cham, Switzerland, 2018; pp. 97–135.
32. Summerscales, J. A review of bast fibres and their composites: Part 4—organisms and enzyme processes. *Compos. Part A Appl. Sci. Manuf.* **2021**, *140*, 106149. [[CrossRef](#)]
33. Bello, S.; Pérez, N.; Kiebist, J.; Scheibner, K.; Ruiz, M.I.S.; Serrano, A.; Martínez, Á.T.; Feijoo, G.; Moreira, M.T. Early-stage sustainability assessment of enzyme production in the framework of lignocellulosic biorefinery. *J. Clean. Prod.* **2021**, *285*, 125461. [[CrossRef](#)]
34. Li, R.; Ye, L.; Mai, Y.-W. Application of plasma technologies in fibre-reinforced polymer composites: A review of recent developments. *Compos. Part A Appl. Sci. Manuf.* **1997**, *28*, 73–86. [[CrossRef](#)]
35. Khan, M.A.; Haque, N.; Al-Kafi, A.; Alam, M.N.; Abedin, M.Z. Jute Reinforced Polymer Composite by Gamma Radiation: Effect of Surface Treatment with UV Radiation. *Polym. Technol. Eng.* **2006**, *45*, 607–613. [[CrossRef](#)]
36. Raj, T.; Kapoor, M.; Semwal, S.; Sadula, S.; Pandey, V.; Gupta, R.P.; Kumar, R.; Tuli, D.K.; Das, B. The cellulose structural transformation for higher enzymatic hydrolysis by ionic liquids and predicting their solvating capabilities. *J. Clean. Prod.* **2016**, *113*, 1005–1014. [[CrossRef](#)]
37. Mercer, J. Improvements in the Preparation of Cotton and Other Fabrics and Other Fibrous Materials. British Patent 13296, 24 October 1850.
38. Rashaduzzaman Mithun, M. Mercerizing Cellulosic Fibres & Its Effects, [Bangladesh] Textile Today, February 2013. Available online: <https://www.coursehero.com/file/69797500/307223027-Mercerizing-Cellulosic-Fibres-Its-Effectsdocx/> (accessed on 11 March 2022).
39. Wada, M.; Nishiyama, Y.; Chanzy, H.; Forsyth, T.; Langan, P. The structure of celluloses. *Powder Diffr.* **2008**, *23*, 92–95. [[CrossRef](#)]
40. Paukszta, D. Mercerisation of rapeseed straw investigated with the use of WAXS method. *Fibres Text. East. Eur.* **2013**, *5*, 19–23. Available online: <http://www.fibtex.lodz.pl/2013/5/19.pdf> (accessed on 11 March 2022).
41. Hand, R.; Ellis, B.; Whittle, B.; Wang, F. Epoxy based coatings on glass: Strengthening mechanisms. *J. Non-Cryst. Solids* **2003**, *315*, 276–287. [[CrossRef](#)]
42. Hernandez Michelena, A. Natural Fibre Reinforced Composite Materials. Ph.D. Thesis, University of Plymouth, Plymouth, UK, 2019. Available online: <https://hdl.handle.net/10026.1/14297> (accessed on 12 March 2022).
43. Anon. Biotex Flax Yarn Technical Data Sheet, Composites Evolution, Chesterfield UK, March 2012. Available online: <https://fdocuments.net/document/biotex-flax-yarn-flax-yarn-technical-data-sheet-march-2012-introduction-biotex.html> (accessed on 11 March 2022).
44. Anon. *Advanced Materials Araldite® LY 1568 Aradur® 3489/Aradur® 3492*; Provisional Technical Data Sheet; Huntsman LLC: The Woodlands, TX, USA, 2010. Available online: https://www.compositesone.com/wp-content/uploads/2013/07/Araldite-LY-1568_Aradur-3489_Aradur-3492_US_e.pdf (accessed on 11 March 2022).
45. Anon. *Advanced Materials: Raise Performance with Building Blocks—Selector Guide for Formulators*; Huntsman Advanced Materials (Switzerland) GmbH: Basel, Switzerland, 2012. Available online: <https://lindberg-lund.no/wp-content/uploads/2018/06/R%C3%A5varer-til-epoksyindustri.pdf> (accessed on 11 March 2022).

46. Summerscales, J.; Searle, T.J. Low-pressure (vacuum infusion) techniques for moulding large composite structures. *Proc. Inst. Mech. Eng. Part L J. Mater. Des. Appl.* **2005**, *219*, 45–58. [[CrossRef](#)]
47. Summerscales, J. Resin Infusion Under Flexible Tooling (RIFT). In *Encyclopedia of Composites*, 2nd ed.; John Wiley & Sons: Hoboken, NJ, USA, 2012; pp. 2648–2658. [[CrossRef](#)]
48. Anon. VAP® Stands for Vacuum Assisted Process; COMPOSYST GmbH: Landsberg am Lech, Germany, 2019; Available online: <https://www.composyst.com/en/vap/> (accessed on 11 March 2022).
49. Curtis, P.T. CRAG Test Methods for the Measurement of the Engineering Properties of Fibre Reinforced Plastics; Technical Report 88 012; Royal Aerospace Establishment: Farnborough, UK, 1988.
50. Summerscales, J.; Virk, A.S.; Hall, W. Fibre area correction factors (FACF) for the extended rules-of-mixtures for natural fibre reinforced composites. *Mater. Today Proc.* **2020**, *31*, S318–S320. [[CrossRef](#)]
51. Mahmood, A.S.; Summerscales, J.; James, M.N. Resin-Rich Volumes (RRV) and the Performance of Fibre-Reinforced Composites: A Review. *J. Compos. Sci.* **2022**, *6*, 53. [[CrossRef](#)]
52. Lu, M.M.; Fuentes, C.A.; Van Vuure, A.W. Moisture sorption and swelling of flax fibre and flax fibre composites. *Compos. Part B Eng.* **2021**, *231*, 109538. [[CrossRef](#)]
53. Khanjanzadeh, H.; Behrooz, R.; Bahramifar, N.; Gindl-Altmutter, W.; Bacher, M.; Edler, M.; Griesser, T. Surface chemical functionalization of cellulose nanocrystals by 3-aminopropyltriethoxysilane. *Int. J. Biol. Macromol.* **2018**, *106*, 1288–1296. [[CrossRef](#)]
54. Kono, H.; Uno, T.; Tsujisaki, H.; Matsushima, T.; Tajima, K. Nanofibrillated Bacterial Cellulose Modified with (3-Aminopropyl)trimethoxysilane under Aqueous Conditions: Applications to Poly(methyl methacrylate) Fiber-Reinforced Nanocomposites. *ACS Omega* **2020**, *5*, 29561–29569. [[CrossRef](#)]
55. Ben-Said, M. Spatial point-pattern analysis as a powerful tool in identifying pattern-process relationships in plant ecology: An updated review. *Ecol. Process.* **2021**, *10*, 56. [[CrossRef](#)]
56. Summerscales, J.; Guild, F.J.; Pearce, N.R.L.; Russell, P.M. Voronoi cells, fractal dimensions and fibre composites. *J. Microsc.* **2001**, *201*, 153–162. [[CrossRef](#)] [[PubMed](#)]
57. Depriester, D.; du Roscoat, S.R.; Orgéas, L.; Geindreau, C.; Levrard, B.; Brémond, F. Individual fibre separation in 3D fibrous materials imaged by X-ray tomography. *J. Microsc.* **2022**. [[CrossRef](#)] [[PubMed](#)]